ELSEVIER

Thermal and MS studies of silver(I) 2,2-dimethylbutyrate complexes with tertiary phosphines and their application for CVD of silver films

I. Szymańska *, P. Piszczek, R. Szczęsny, E. Szłyk

Nicolaus Copernicus University, Faculty of Chemistry, 87 100 Toruń, Poland

Abstract

$[Ag_2(CH_3CH_2C(CH_3)_2COO)_2]$ (**1**), $[Ag_2(CH_3CH_2C(CH_3)_2COO)_2(PMe_3)_2]$ (**2**) and $[Ag_2(CH_3CH_2C(CH_3)_2COO)_2(PEt_3)_2]$ (**3**) were prepared and characterized by MS-EI; ^1H, ^{13}C, ^{31}P NMR, variable temperature IR (VT-IR) spectroscopy and thermal analysis. MS and VT-IR data analysis suggests bidentate bridging carboxylates and monodentately bonded phosphines in the solid phase. The same methods used for gas phase analysis of **1–2** proved $[(CH_3CH_2C(CH_3)_2COO)Ag_2]^+$ as the main ion, which could be transported in the gas phase during the CVD process. In the case of **3**, similar intensity to the latter ion revealed $[Ag\{P(C_2H_5)\}]^+$ and it is responsible for the CVD performance of **3**. Thermal analysis results revealed that decomposition of **1–3** proceed in one endothermic process, with metallic silver formation between 197 and 220 °C. In the case of **1**, VT-IR studies of the gaseous decomposition products demonstrate the presence of ester molecules and CO_2, whereas for **2** the main gaseous product appeared to be acid anhydride. Therefore, **2** was not used as a silver CVD precursor. Metallic layers were produced from **3** in *hot-wall* CVD experiments, (between 200 and 280 °C), under a total reactor pressure of 2.0 mbar, using argon as a carrier gas. Thin films deposited on Si(111) substrate were characterized by X-ray diffraction (XRD), scanning electron microscopy (SEM) and atomic force microscopy (AFM). Silver films obtained at moderate temperature (220–250 °C) revealed a thickness below 50 nm, and were whitish colored and slightly matt.

© 2007 Elsevier Ltd. All rights reserved.

Keywords: Ag(I) complexes; Phosphine; Carboxylates; Thermal properties; MS; CVD

1. Introduction

In recent years silver(I) carboxylates and their complexes with tertiary phosphines have found application as precursors for Chemical Vapor Deposition (CVD) [1–4]. The produced silver thin layers can be applied in contacts for ULSI microelectronic circuits, catalysis, or as a dopant in fabrication of high-temperature superconductors and other applications [2]. The precursors should be volatile and decompose at relatively low temperatures in the CVD apparatus. Therefore, knowledge about thermal properties of the precursors is important for the evaporation of metallated species and deposition on substrates. It has been noted that the volatility of complexes is improved in the case of bulky peripheral substituents and perfluorinated ligands. There-

fore, the silver precursors most often used in CVD are organometallics or β-diketonates complexes with tertiary phosphines (PMe_3 [3,5], PEt_3 [3,5]), silylated alkenes [6], alkynes [7,8] and recently carboxylates [4,9]. Out of the latter ones, volatile perfluorinated and aliphatic Ag(I) carboxylates and their complexes with tertiary phosphines have been reported [4,10,11]. The majority of Ag(I) carboxylates appeared to be dimers with bridging RCOO groups [9]. However, for $[Ag(O_2CCH_3)(PBu^t_3)]$ and $[Ag(O_2CCH_3)(PPh_3)_2]$ symmetrical chelating carboxylates were detected, whereas in the case of $[Ag(OOCH)(PPh_3)_2]$ monodentately bonded formate was reported [9,12–14]. The studied, silver(I) carboxylates were thermally stable, and decompose to metallic silver in a wide temperature range [15–17]. In CVD experiments, knowledge about the metallated species transported in the gas phase is fundamental for deposition process control [18–20]. The gaseous products transported in a CVD reactor, should include the metal ion and be

* Corresponding author. Tel.: +48 56 611 4317; fax: +48 56 654 2477.
  E-mail address: pola@chem.uni.torun.pl (I. Szymańska).

stable in the gas phase until deposition on the substrate. Therefore, temperature variable MS and TGA-IR spectra of the gases evolved during the decomposition processes will be described in the presented paper. Data from the latter studies will be use for elaboration of the fragmentation schemes. Moreover, the fragmentation schemes of coordinated ligands, should provide unique knowledge about the chemistry of silver(I) complexes in the gas phase. The article is also intended to describe a mechanism of carboxylates thermal decomposition, therefore VT-IR spectra were measured and discussed.

2. Experimental

2.1. Chemicals and instrumentation

$CH_3CH_2C(CH_3)_2COOH$ (97%), trimethylphosphine (PMe_3) (1 M solution in THF), triethylphosphine (PEt_3) (1 M solution in THF), triethylorthoformate (TEOF) were purchased from Aldrich, $AgNO_3$, $NaHCO_3$ and C_2H_5OH were purchased from POCh (Poland), and all compounds were used as received. Ethanol was dried by standard methods.

Thermal studies (TG, DTG, DTA) were performed on a SDT 2960 TA analyser. Decomposition processes were studied in a dynamic atmosphere of dry nitrogen flowing at 40 ml min^{-1}, heating rate 2.5 °C min^{-1}, heating range up to 400 °C and sample mass 2–5 mg. Gaseous products of thermal decomposition were detected by a FT IR Bio-Rad Excalibur spectrophotometer equipped with a thermal connector for gases evolved from a SDT 2960 TA analyser. The thermal connector was heated to 200 °C. Powder X-ray diffraction data for the thermal analysis residues were obtained with a Philips X'PERT diffractometer using Cu Kα radiation. Variable temperature mass spectra were registered using a Finnigan MAT 95 spectrometer with the EI technique (heating range 30–300 °C). ^1H and ^{13}C NMR spectra in CD_3CN or C_6D_6 were collected with a Varian Gemini 200 MHz spectrometer using TMS as the standard, and 85% H_3PO_4 for ^{31}P NMR (80.96 MHz). IR spectra were recorded using a Perkin–Elmer 2000 FT IR spectrometer in the range 4000–400 cm^{-1}, in KBr discs. Variable temperature IR (VT-IR) studies in the solid phase were carried out with a SPECAC (Perkin–Elmer) temperature variable cell. The composition of vapors formed during the thermolysis of the studied compounds was determined by VT-IR spectroscopy. Spectra of vapors transported with the carrier gas (Ar) were recorded using the equipment as reported [21]. Silver was determined argentometrically (after complex mineralization), whereas C, H, P were determined by elemental microanalysis.

2.2. Synthesis

2.2.1. [Ag$_2$(CH$_3$CH$_2$C(CH$_3$)$_2$COO)$_2$] (1)

2,2-Dimethylbutyric acid (3.5 mmol) and potassium nitrate (0.43 mmol) were suspended in a water–ethanol solution (1:1), heated to 40 °C and stirred 1 h, followed by silver nitrate (3.5 mmol) addition (all manipulations were carried out in the darkness). The obtained precipitate was filtered, washed with water, ethanol and dried. *Anal.* Calc. for $C_{12}H_{22}Ag_2O_4$: C, 32.2; H, 5.0; Ag, 48.3. Found: C, 32.0; H, 5.2; Ag, 48.7%. IR: 1555, 1477, 1405, 1366, 1357, 1290 cm^{-1}; ^1H NMR (CD_3CN): 0.83 ppm (3H, t, CH_3), 1.10 ppm (6H, s, CH_3), 1.49 ppm (2H, q, CH_2); ^{13}C NMR (CD_3CN): 10.3 ppm (CH_3), 26.9 ppm (CH_3)$_2$, 35.5 ppm (CH_2), 44.7 ppm (C), 183.9 ppm (COO).

2.2.2. [Ag$_2$(CH$_3$CH$_2$C(CH$_3$)$_2$COO)$_2$(PMe$_3$)$_2$] (2) and [Ag$_2$(CH$_3$CH$_2$C(CH$_3$)$_2$COO)$_2$(PEt$_3$)$_2$] (3)

Complexes were synthesized, in dried argon, using Schlenk techniques, in the darkness. In a general procedure: **1** (4 mmol) in C_2H_5OH (40 cm^3) was mixed with 5 cm^3 of TEOF and PR$_3$ (4 mmol) (THF solution), where R = Me, Et. The mixture was stirred at room temperature for 4 h, filtered and solvents evaporated on a vacuum line. [Ag$_2$(CH$_3$CH$_2$C(CH$_3$)$_2$COO)$_2$(PMe$_3$)$_2$] (**2**) was obtained as white crystals, which were recrystallized from ethanol, whereas [Ag$_2$(CH$_3$CH$_2$C(CH$_3$)$_2$COO)$_2$(PEt$_3$)$_2$] (**3**) was obtained as a green–yellow oil and was analyzed directly after evaporation. *Anal.* Calc. for $C_{18}H_{40}Ag_2O_4P_2$ (**2**): C, 36.1; H, 6.7; P, 10.3; Ag, 36.1. Found: C, 36.3; H, 6.9; P, 10.2; Ag, 36.4%. IR: 1550, 1472, 1399, 1359, 1286, 960 cm^{-1}. ^1H NMR (CD_3CN, ppm): 0.81 (3H, t, CH_3), 1.03 (6H, s, CH_3), 1.34 (9H, d, PCH_3), 1.46 (2H, q, CH_2); ^{13}C NMR (CD_3CN, ppm): 9.7 (CH_3), 14.8 P(CH_3), 26.1 (CH_3)$_2$, 34.6 (CH_2), 43.0 (C), 184.4 (COO); ^{31}P NMR (CD_3CN, ppm): −35.4.

Anal. Calc. for $C_{24}H_{52}Ag_2O_4P_2$ (**3**): C, 42.2; H, 7.7; P, 9.1; Ag, 31.6. Found: C, 42.3; H, 7.4; P, 9.0; Ag, 31.1%. IR: 1549, 1458, 1405, 1364, 1045, 764 cm^{-1}. ^1H NMR (CD_3CN, ppm): 0.84 (3H, t, CH_3), 1.07 (6H, s, CH_3), 1.18 (9H, t, PEt_3), 1.47 (2H, q, CH_2), 1.69 (2H, q, PEt_3). ^{13}C NMR (CD_3CN, ppm): 9.19 (CH_3), 10.5 P(CH_2CH_3), 16.9 P(CH_2CH_3), 26.8 (CH_3)$_2$, 35.0 (CH_2), 43.6 (C), 185.8 (COO); ^{31}P NMR (CD_3CN, ppm): 28.2.

2.3. CVD experiments

The deposition experiments were carried out using horizontal *hot-wall* CVD reactor as described [11]. Silver films were deposited on Si(111) and steel substrates, under 2 mbar, and in the deposition temperature 200–280 °C. The films were characterized by X-ray diffraction (XRD). XRD data were collected with a Philips X'PERT diffractometer, in 30–80° 2Θ ranges, using CuKα irradiation and sample spinning (step size – 0.1°, program. res. slit – 0.5, measuring time – 11 s per point). The silver films' morphology were studied by a scanning electron microscopy (SEM – LEO 1460 V) and an atomic force microscopy instrument (Veeco, Multimode, Nanoscope IIIa Controler, Taping Mode AFM).

3. Results and discussion

3.1. Preparation

All silver compounds were synthesized in the darkness. Silver 2,2-dimethylbutyrate **1** was obtained by the reaction of 2,2-dimethylbutyric acid and silver nitrate in a 1:1 ratio in a water–ethanol solution. This reaction is fast and the white product can be simply isolated. Both silver 2,2-dimethylbutyrate complexes with phosphines $[Ag_2(CH_3CH_2C(CH_3)_2COO)_2(PMe_3)_2]$ (**2**) and $[Ag_2$-$(CH_3CH_2C(CH_3)_2COO)_2(PEt_3)_2]$ (**3**) were synthesized by the direct reaction of silver carboxylate and the respective phosphine in a 1:1 ratio, using ethanol as solvent and in dried argon. **2** was obtained as white crystals, which were recrystallized from ethanol, whereas **3** was a green–yellow oil.

3.2. IR and NMR spectra

Table 1 demonstrates characteristic absorption bands in the IR spectra, which can be assigned to the stretching modes of the COO group. Carboxylates can coordinate in many modes such as: unidentate, chelating or bridging bidentate [22–24]. The carboxylate coordination can be proposed by analysis of the parameter $\Delta v_{COO} = v_{asym} - v_{sym}$, calculated for studied compounds and identical sodium salts. In the case of silver 2,2-dimethylbutyrate the COO bands were detected at: $v_{asym} = 1548$ cm^{-1}, $v_{sym} = 1405$ cm^{-1}. For complexes **2** and **3** Δv_{COO} was 153 cm^{-1} and 159 cm^{-1}, respectively, which suggest similar coordination as for **1**. The calculated Δ parameters for the discussed compounds are bigger than those for the appropriate sodium salts. This fact suggests a bridging coordination mode of the carboxylic group and a polymeric structure [9,25]. Absorption bands of phosphines derived from P–C stretching vibrations are shifted for **2** by 32 cm^{-1} and for **3** by 19 cm^{-1} in comparison to the free phosphines, which confirms the coordination of the ligands [26,27].

The ^{13}C and ^{31}P NMR spectral chemical shifts of **1–3** are listed in Table 2. One might expect that the ^{13}C signal of the COO carbon should give the most significant changes upon coordination. However, the ^{13}C NMR spectra of **1–3** revealed the COO carbon line at 184.0–185.8 ppm, with a coordination shift (0.9–2.7 ppm) downfield in comparison to the free acid spectra. In the case of perfluorinated silver carboxylates, this signal was observed at higher field (159.1–165.7 ppm) [32]. The observed chemical shifts suggest an opposite effect on the COO carbon due to the

inductive effect imposed by the fluorine atoms. However, the coordination shifts of the COO carbon in perfluorinated carboxylates (∼1 ppm) were similar to the value calculated for **1**, which reveal comparable silver–carboxylate interactions for fluorinated and non-fluorinated silver salts. In the case of complexes **2** and **3**, the carbonyl carbon exhibited weak singlets at 184.4 and 185.8 ppm, respectively. For $[Ag_2(PPh_3)_2(\mu\text{-}RCOO)_2]$, R – aliphatic chain and $[Ag(PPh_3)(RCOO)]$, R – silylated radical, COO singlets were detected in the range 180.8–187.7 ppm [28,29]. However, in the case of silver complexes with perfluorinated carboxylates $[Ag_2(PR'_3)_2(\mu\text{-}RCOO)_2]$ (R' = Me, Et), resonances of COO were observed upfield (161.3–163.2 ppm) [30,34]. The coordination shifts for **2** of 1.3 and **3** of 2.7 ppm were close to the values calculated for the compounds $[Ag_2(PR'_3)(RCOO)]$. Therefore, the bridging mode of the silver–carboxylate linkage in $[Ag_2(PR'_3)$-$(RCOO)]$ salts can be similar for aliphatic, silylated and perfluorinated carboxylates. Single ^{31}P resonances appeared at −35.4 **2** and 28.2 ppm **3** – Table 2. The values of chemical and coordination shifts for **2** are close to those observed for perfluorinated carboxylate complexes $[Ag_2(PMe_3)_2$-$(\mu\text{-}RCOO)_2]$. However, for **3** only the coordination shift is similar to the value registered for $[Ag_2(PEt_3)_2(\mu\text{-}RCOO)_2]$, but the signal was detected at higher fields (13.5–13.1 ppm) [30,34].

3.3. Analysis of variable temperature IR spectra

An application of **1–3** as CVD precursors requires determination of their thermal stability and composition of the vapors formed during their thermolysis. Therefore variable temperature IR (VT-IR) studies have been carried out and the results are presented in Figs. 1–4. IR spectra of **1–3**, registered between 20 and 250 °C, revealed differences in the mechanism of their thermal decomposition (Fig. 1). In the case of **1** and **2**, the thermolysis proceeds with complete decomposition of these compounds. Bands registered at 1676, 1608 cm^{-1} **1** and 1680, 1598 cm^{-1} **2**, at 250 °C,

Table 2
^{13}C, ^{31}P NMR spectral analysis data [ppm]

Compound	^{13}C		^{31}P	
	δ COO	Δ_1	δ	Δ_2
$[Ag_2(CH_3CH_2C(CH_3)_2COO)_2]$ (**1**)	184.0	0.9		
$[Ag_2(CH_3CH_2C(CH_3)_2COO)_2(PMe_3)_2]$ (**2**)	184.4	1.3	−35.4	24.9
$[Ag_2(CH_3CH_2C(CH_3)_2COO)_2(PEt_3)_2]$ (**3**)	185.8	2.7	28.2	46.3

$\Delta_1 = \delta$ COO(complex) − δ COO(acid); δ COO(acid) = 183.1 ppm.
$\Delta_2 = \delta - \delta$ PR_3; $\delta(PMe_3) = -60.3$ ppm; $\delta(PEt_3) = -18.1$ ppm.

Table 1
Selected IR band (cm^{-1}) of the studied compounds

Compound	v_{as}(COO)	v_s(COO)	Δv(COO)	v(P–C)
$[Ag_2(CH_3CH_2C(CH_3)_2COO)_2]$ (**1**)	1548	1405	143	
$[Ag_2(CH_3CH_2C(CH_3)_2COO)_2(PMe_3)_2]$ (**2**)	1549	1396	153	740
$[Ag_2(CH_3CH_2C(CH_3)_2COO)_2(PEt_3)_2]$ (**3**)	1553	1394	159	689

$\Delta v_{COO(sodium\ salt)} = 119$ cm^{-1}.
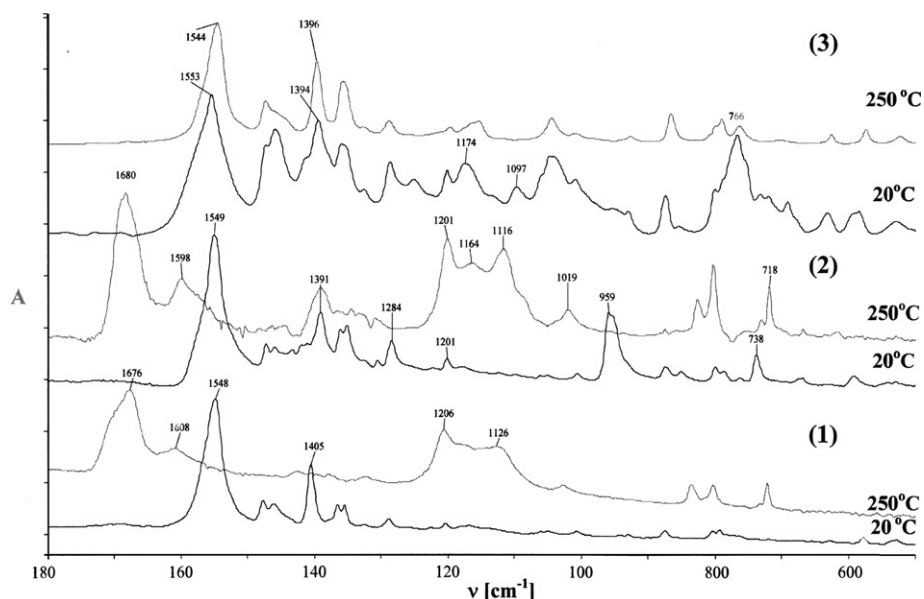
Fig. 1. Variable temperature IR spectra of **1**–**3**, registered at 20 and 250 °C.
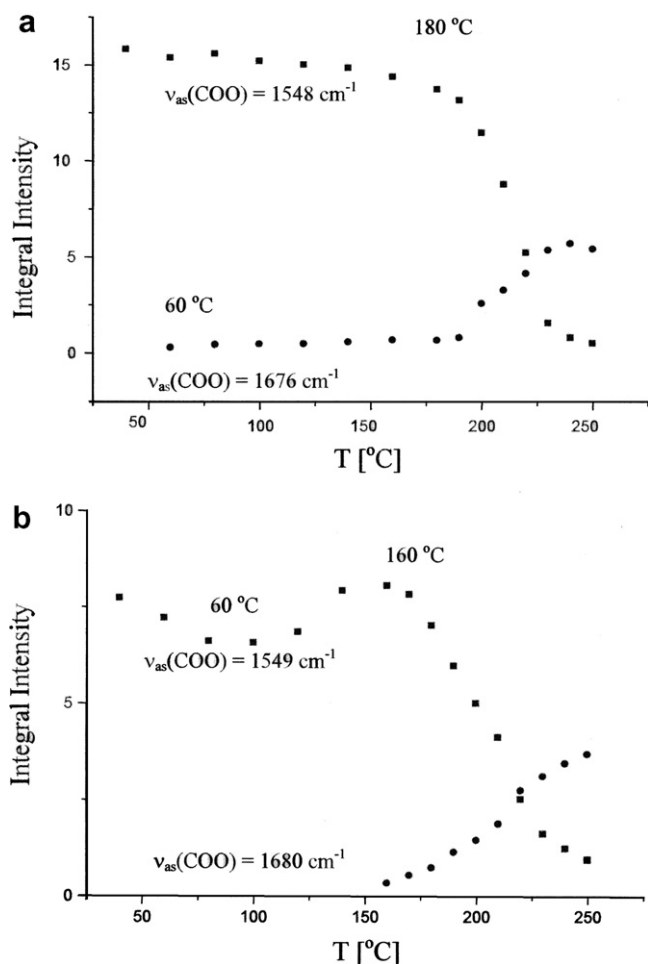
Fig. 2. Temperature dependence of the integral intensity of bands assigned to $v_{as}(COO)$ and $v(CO)$, observed between 1480 and 1800 cm^{-1}, in spectra of **1** (a) and **2** (b).

suggest formation of a different type of Ag–OOCR linkage in the solid residue than at room temperature. Calculated Δv parameters exhibit the increase from 208 to 252 cm^{-1} for **1** and from 239 to 291 cm^{-1} for **2**, in comparison to spectra registered at 20 °C (Table 1). The latter suggests decomposition of the polymeric structure of **1** and **2**, where carboxylate ligands form *syn–syn* bidendate bridges, and the formation of another type of Ag(I) interaction with the carboxylate ligands [22,23].

The differences in the decomposition pathway of **1** and **2** are also observed on the plot of integral intensity of $v_{as}(COO)$ bands versus temperature (Fig. 2). The relatively high thermal stability of **1** can be noted between 40 and 180 °C. However, the presence of a weak band at 1676 cm^{-1} suggests decomposition process onset at 60 °C. Above 180 °C a rapid increase of this band's intensity is observed, while the $v_{as}(COO) = 1548$ cm^{-1} band reveals the opposite effect. The latter can be related to complete decomposition of **1** with the evolution of carboxylic acid. Between 180 and 230 °C (Fig. 3) the main components of the gas phase of **1** are: CO_2 (2359, 667 cm^{-1}), ester species ($v_{C=O} = 1767$, $\delta_{OCO} = 1116$ cm^{-1}), and fragments containing carboxylate acid groups ($v_{OH} = 3520$, $v_{C=O} = 1716$ cm^{-1}). Bands that could be assigned to volatile silver–carboxylate species were not found, which confirms the postulated decomposition pathway by DTA/TGA studies. The latter is in favor of decomposition of **1** leaving silver containing species in the solid phase.

For **2**, the dependence of the integral intensity of v_{as}-(COO) bands versus temperature changes stepwise, exhibiting the first step at 60 °C, with the second one at 160 °C (Fig. 2b). Simultaneously CH_3 librational modes (rocking and/or wagging) at 959 cm^{-1} and $v(P–C)$ (738 cm^{-1}) bands
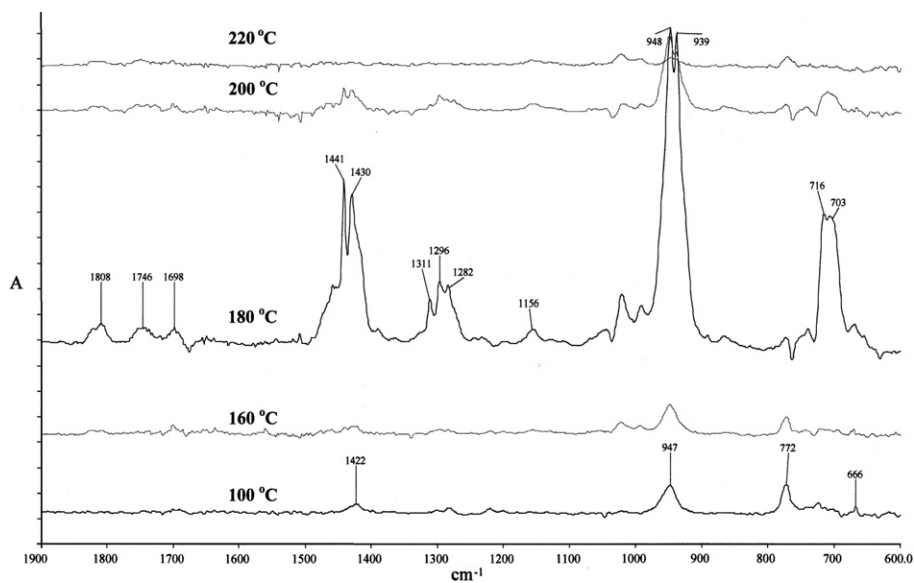
Fig. 3. VT-IR spectra of vapors formed during the thermal decomposition of **2**.
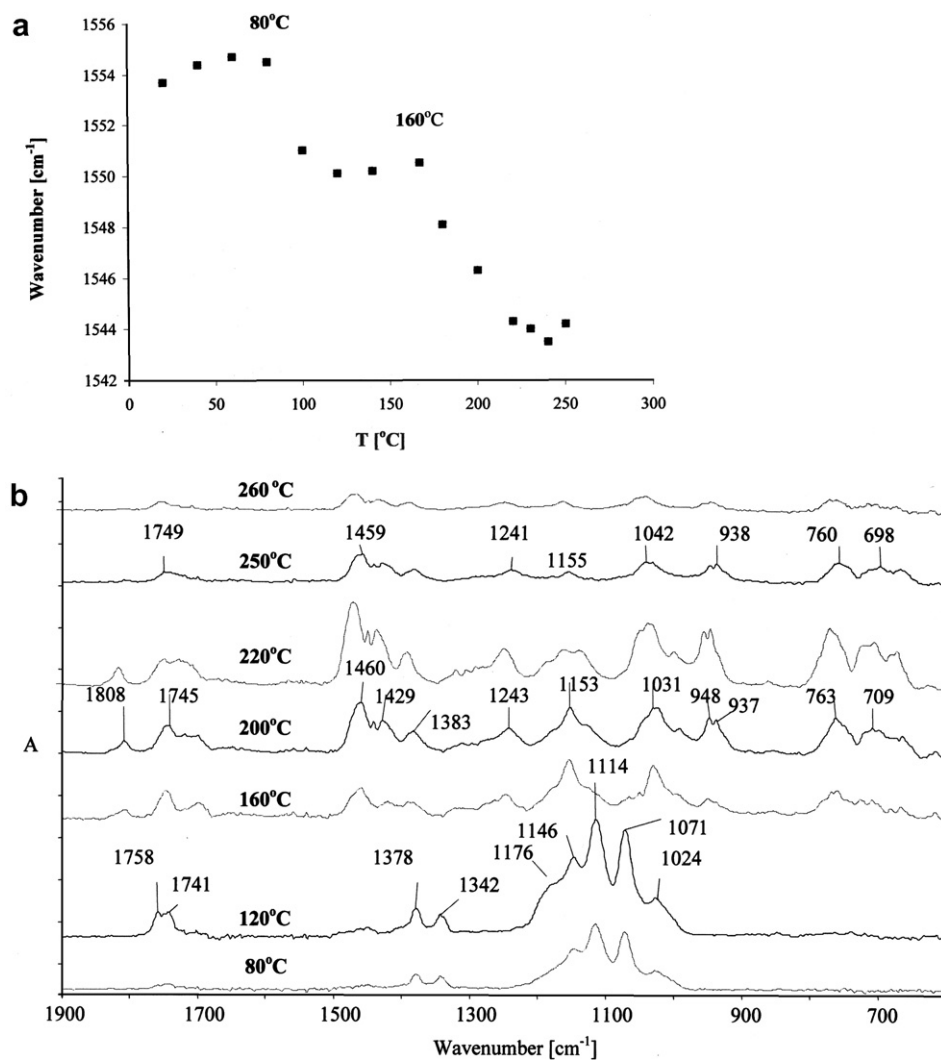
Fig. 4. The dependence of the frequency of v_{as}(COO) motions vs. temperature (a), and changes of the vapor composition during the thermal decomposition of **3** (b).

revealed intensity decrease. Hence, the phase transition at lower temperatures can be attributed to phosphine detachment from **2**. The same as for **1**, the main decomposition product appears to be Ag(I) carboxylate intermediates. However, their complete decomposition processes was observed above 160 °C, (bands at 1680 and 1549 cm^{-1}), which indicate low thermal stability of these species.

Analysis of vapors spectra, registered in the range 160 and 200 °C, revealed phosphine bands: $\delta(CH_2)$ 1430–1441 cm^{-1}, $\delta_{sym}(CH_3)$ 1282–1311 cm^{-1}, $\delta(CH_3)$ 939–948 cm^{-1} and $\nu_{asym}(P–C)$ 703–716 cm^{-1}. The latter is in favor of phosphine species (PCH$_2$, PCH$_3$), which are predominant in the vapors of **2**. Besides that, weak bands observed in the range 1698–1808 cm^{-1}, (registered at 180 °C), can be assigned to a volatile acid anhydride (1808, 1746 cm^{-1}) and aliphatic carboxylate (1698 cm^{-1}).

Comparison VT-IR and MS data confirms the proposed decomposition mechanism of **2**. According to MS data (Table 3), the complete decomposition of **2**, proceeds between 80 and 260 °C, with volatile species formation. The main constituents are: [PH(CH$_3$)]$^+$, [P(CH$_3$)$_2$]$^+$ and [P(CH$_3$)$_3$]$^+$ fragments, whereas only trace quantities of [AgP(CH$_3$)$_3$]$^+$ were noticed. Carboxylate silver bonded fragments (e.g. [Ag$_2$(OOCC(CH$_3$)$_2$CH$_2$CH$_3$)]$^+$) were not observed in the vapors. This can be explained by the low stability of species containing the above fragments and their rapid decomposition.

In comparison to **1** and **2**, the thermolysis pathway of **3** is different (Fig. 1). The dependence between frequency of $\nu_{asym}(COO)$ bands and temperature (Fig. 4a) suggests that the decomposition pathway of **3** proceed in two stages, with the first step near 80 °C and second one at 160 °C. Moreover, significant differences in the vapors composition in the temperature ranges 60–140 °C and 160–260 °C were

observed (Fig. 4b). Species containing ester groups (1741, 1758, and 1176 cm^{-1}) and aliphatic ethers (group of bands between 1024 and 1146 cm^{-1}) were the main volatile components at lower temperatures. Above 160 °C, the composition of the vapors changes and bands at 763, 1031, 1243 and 1460 cm^{-1} indicate the presence of Ag–phosphine derivatives as the main volatile decomposition products. When compared to the room-temperature spectrum of **3** the bands assigned to Ag–PEt$_3$ groups are almost identical (766, 1046, 1250 and 1459 cm^{-1}). Simultaneously, absorption bands derived from volatile species containing Ag–OOCR fragments were not observed. In the temperature range 160–260 °C, only bands from acid anhydride (1745, 1808 cm^{-1}) and ester derivatives (1153, 1720–1750 cm^{-1}) were noticed.

According to the VT-IR results it can be concluded that **1** and **2** are not suitable precursors for CVD of silver, due to their low thermal stability in the temperature range 20–250 °C. In contrast, the formation of volatile and stable silver–phosphine intermediates between 160 and 260 °C during the decomposition of **3** suggests its potential usability as a Ag CVD precursor, as was confirmed by CVD experiments (*vide infra*).

3.4. Mass spectra analysis

Variable temperature mass spectra were studied to detect the metallated species, which can be transported in the gas phase during precursor heating in a CVD process. EI-MS spectra of **1**, **2** and **3** were recorded in the range 30–300 °C and the results are listed in Table 3. The following most intensive organic ions: [CH$_3$CH$_2$CH$_2$]$^+$, [CH$_3$CH$_2$C=CH$_2$]$^+$ and [CH$_3$CH$_2$C(CH$_3$)$_2$]$^+$, as well as [COO]$^+$ and [COOH]$^+$, were detected in the studied tem-

Table 3
Mass spectra analysis data

Fragmentation ion	m/z	Compound/Temperature/Int. (%)						
		1	**2**			**3**		
		197 (°C)	86 (°C)	107 (°C)	256 (°C)	116 (°C)	182 (°C)	245 (°C)
[CH$_3$CH$_2$CH$_2$]$^+$	43	100	15.1	13.6	100	56.6	100	93.8
[COO]$^+$	44	23.3	21.4	14.8	40.8	12.4	24.2	22.1
[COOH]$^+$	45	7.9	71.6	46.1	9.4	17.7	16.7	5.9
[(CH$_3$)HP]$^+$	47	xxx	23.9	12.7		xxx	xxx	xxx
[CH$_3$CH$_2$C=CH$_2$]$^+$	55	31.0	4.8	4.2	60.0	25.4	36.8	33.2
[CH$_3$CH$_2$CHCH$_2$]$^+$	56	6.8	12.2	8.0	10.2	7.7	8.7	5.9
[(CH$_3$)$_2$P]$^+$	61	xxx	100	100		xxx	xxx	xxx
[CH$_3$CH$_2$C(CH$_3$)=CH$_2$]$^+$	70	9.0	1.1	1.1	15.3	5.3	9.1	11.1
[CH$_3$CH$_2$C(CH$_3$)$_2$]$^+$	71	63.8	7.3	6.5	79.6	30.0	50.0	65.3
[(CH$_3$)$_3$P]$^+$	76	xxx	83.6	44.9		xxx	xxx	xxx
[(C$_2$H$_5$)$_2$HP]$^+$	90	xxx	xxx	xxx	xxx	55.6	30.5	
[Ag]$^+$	107	2.0			4.1			
[(C$_2$H$_5$)$_3$P]$^+$	118	xxx	xxx	xxx	xxx	27.3	14.9	
[AgP(CH$_3$)$_3$]$^+$	183	xxx	2.6	3.5		xxx	xxx	xxx
[Ag$_2$]$^+$	216	9.5			10.6			7.2
[AgP(C$_2$H$_5$)$_3$]$^+$	225	xxx	xxx	xxx	xxx	77.3	57.9	
[(CH$_3$CH$_2$C(CH$_3$)$_2$COO)Ag$_2$]$^+$	331	38.3			81.8	4.5		56.7

xxx, unable to observe.

perature range. Moreover, analysis of the spectra revealed the presence of certain metallated species formed in the strictly defined temperature ranges. The spectrum of **1** (at 197 °C) exhibited $[(CH_3CH_2C(CH_3)_2COO)Ag_2]^+$ (R.I. = 38%) as the most intensive signal. Similar disilver species were observed in MS spectra of perfluorinated and aliphatic non-fluorinated silver carboxylates [20,31]. The latter silver(I) salts form dimers or aggregates of these dimers in the solid phase with bridging carboxylates, and likewise the same can be suggested for **1**. The observed silver bonded species can be formed by detachment of RCOO˙ at the temperature characteristic for the studied precursor (e.g. 197 °C for **1**). In the next stage, the $[(CH_3CH_2C(CH_3)_2COO)Ag_2]^+$ fragment decomposes to Ag_2^+ and organic ions, which is evident from the characteristic line pattern for Ag_2^+ [3 lines, R.I. = 1:1.860:0.865, natural isotopic abundance of ^{107}Ag (51.4%) and ^{109}Ag (48.6%)].

In the case of **2** between 30 and 120 °C the following phosphorous containing species $[(CH_3)_2P]^+$ (R.I. = 100% at 86 °C and 107 °C), $[(CH_3)_3P]^+$ (R.I. = 84% at 86 °C; R.I. = 45% at 107 °C), $[(CH_3)_2HP]^+$ (R.I. = 24% at 86 °C; R.I. = 13% at 107 °C) and $[Ag(PCH_3)]^+$ (R.I. = 2.6% at 86 °C; R.I. = 3.5% at 107 °C) were detected. These phosphorous embodied fragments are in favor of trimethylphosphine detachment and complex decomposition in the 30–120 °C range. At higher temperatures (160–240 °C), the desirable metallated ions $[(CH_3CH_2C(CH_3)_2COO)Ag_2]^+$ (R.I. = 82% at 220 °C), $[Ag_2]^+$ (R.I. = 11% at 220 °C) and $[Ag]^+$ (R.I. = 4% at 220 °C) appeared (Fig. 5). Fragments detected in the spectrum of **2** (30–300 °C) suggest detachment and fragmentation of trimethylphosphine followed by RC–COO bond dissociation (absence of RCOO and RCO ions) [31]. The latter causes silver bonded species formation, which decompose in the last stage to Ag_2^+ and Ag^+ (Fig. 5).

Fig. 5. Fragmentation scheme for $[Ag_2(CH_3CH_2C(CH_3)_2COO)_2(PMe_3)_2]$ (**2**).

In the case of **3**, below 200 °C, phosphorous containing metallated fragments $[AgP(C_2H_5)_3]^+$ (R.I. = 77% at 116 °C; R.I. = 15% at 182 °C) were registered, which suggest a stronger Ag–P bond in comparison to the trimethylphosphine complex **2**. Phosphine bonded fragments are less desirable in CVD of metals, due to possible increase of film contamination with P. The $[Ag_2]^+$ signals revealed similar intensity (R.I. = 10%) for both complexes, whereas $[Ag]^+$ appeared only for **2**. The above demonstrate that the most stable volatile silver coordinating fragment for **1–3** is the $[(CH_3CH_2C(CH_3)_2COO)Ag_2]^+$ ion.

In the case of complex **2** abundance of $[(CH_3CH_2C(CH_3)_2COO)Ag_2]^+$ ion was twofold higher than for **3**, which corresponds to the detachment of the PR_3 from **2** in the first stage. For **3** the lower relative intensity of $[(CH_3CH_2C(CH_3)_2COO)Ag_2]^+$ can be related to the presence of the stable phosphine (PEt_3) bonded silver(I) ions. The formation of $[AgP(C_2H_5)_3]^+$ and other similar ions can be explained by higher stability of the Ag–P bond, coming from the stronger σ-electron donor character of PEt_3 than PMe_3.

Above results demonstrate that compounds **1**, **2** and **3** can be used for the deposition of silver layers using the CVD method, due to formation of the volatile metallated species (e.g. $[(CH_3CH_2C(CH_3)_2COO)Ag_2]^+$, $[AgP(C_2H_5)_3]^+$).

3.5. Results of thermal analysis (TGA/DTG/DTA)

Thermal properties of the studied compounds are also important for the assessment of their future usage in CVD of silver layers. The temperature of decomposition process onset and temperature of silver formation are two factors which determine CVD procedure parameters. The results of thermal analysis are listed in Table 4 [10]. Salt **1** decomposes in one endothermic process (onset = 125 °C, maximum rate of reaction = 198 °C). The mass loss on the TG curve corresponds to detachment of carboxylate and the final residue is metallic silver formed at $T_f = 208$ °C. The observed silver formation temperature is below 250 °C, which makes **1** a promising precursor for hot-wall CVD of silver layers. When comparing **1** to perfluorinated silver(I) carboxylates it is evident that they decompose at higher temperatures (e.g. $CF_3(CF_2)_2COOAg$; $T_f = 470$ °C) [32]. The latter suggests that perfluorinated ligands revealed improved volatility, but they are more thermally stable then branched non-fluorinated carboxylates. In the case of **2** and **3** one endotherm was also observed on the DTA, with onset temperatures of 164 °C and 170 °C, respectively. The onset temperatures are almost in the range of instrument accuracy; hence one may presume that decomposition starts with the partial dissociation of the carboxylate residue, which has further evidence in the MS spectra of **1–3**. Analysis of the TG curves indicates mass losses which correspond to the detachment of carboxylate residue and phosphine in the same endothermic reaction. The maximum reaction rates (DTG) were detected at 205 °C and 250 °C, respectively, which confirms
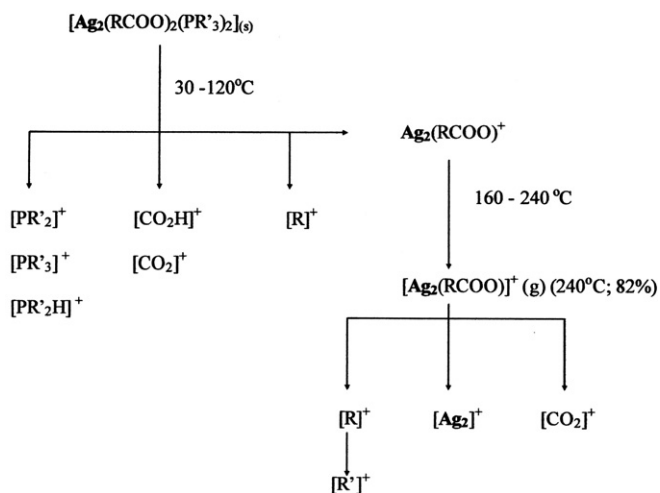
Table 4
Thermal analysis results

Compound	Heat effect on DTA	Temperature (°C)			Residue (%)	
		T_{init}	T_{max}	T_f	Calc.	Found
$[Ag_2(CH_3CH_2C(CH_3)_2COO)_2]$ (**1**)	Endo	125	197	208	48.4	52.9
$[Ag_2(CH_3CH_2C(CH_3)_2COO)_2(PMe_3)_2]$(**2**)	Endo	50	205	206	36.1	35.5
$[Ag_2(CH_3CH_2C(CH_3)_2COO)_2(PEt_3)_2]$ (**3**)	Endo	60	250	290	31.6	32.8

T_{init}, initial temperature; T_{max}, maximum temperature; T_f, final temperature.

MS observations that PEt$_3$ forms a stronger Ag–P σ-donor, π-acceptor bond than PMe$_3$. A similar phenomenon was observed for $[Au(RCOO)(PR_3)]$ and $[Ag(RCOO)(PR_3)]$ complexes with the studied phosphines and perfluorinated carboxylates [30,34]. The decomposition reaction was completed at: T_f **2** = 206 °C, T_f **3** = 290 °C. In both cases, metallic silver was confirmed by TG calculations and detected by XRD studies of the residue in the crucible. The observed diffractogram lines (0.2352, 0.2026, 0.1179, 0.1444, 0.1233 nm) correspond to metallic silver (Powder Diffraction File) [33]. Temperatures of silver formation are accept for CVD purposes with the heating device working below 300 °C.

Considering decomposition mechanism of **2** and **3**, one can propose simultaneous or very close in time, consecutive carboxylate residue and phosphine detaching reactions. In comparison to the reported silver perfluorinated carboxylates complexes with PPh$_3$ (T_f = 219–340 °C), the studied complexes exhibited significantly lower temperatures of silver formation [34]. The latter makes them much more promising CVD precursors of metallic silver than analogues with heavier (aromatic) phosphines.

Analysis of the IR spectra of the gases evolved during the thermal decomposition of **1** suggest the presence of acid ($v_{(OH)}$ = 3577 cm^{-1}, C–H stretching at 2967 cm^{-1}, $v_{(C=O)}$ = 1752 cm^{-1}, $v_{(C-O)}$ = 1258 cm^{-1}, $\delta_{(O-C=O)}$ = 668 cm^{-1}) which was also detected in the gaseous products of the silver acetate thermal decomposition reaction [17].

TGA/IR studies of the gas phase from decomposition reactions of **2** and **3** revealed the characteristic absorption bands for acid anhydride ($v_{a(COO)}$ = 1816 cm^{-1}, $v_{s(COO)}$ = 1759 cm^{-1}) (Fig. 1). Moreover, bands typical for the phosphines were observed.

3.6. Results of CVD experiments

Silver films were deposited using precursor **3** and *hot-wall* CVD equipment. The substrates were Si(1 1 1) and steel plates, at a deposition temperature between 200 and 280 °C, under 2.0 mbar of the total reactor vaccum, in argon atmosphere. The vaporization temperature was fixed at 170 °C for CVD experiments resulting in an efficiency of 75–83%. The fabricated silver films revealed thickness below 50 nm, and were whitish colored and slightly matt. Variation of the deposition temperature and the amount of precursor used in the CVD experiments (100–300 mg) appeared to be the main parameters which have an impact on the thickness of the silver layers.

Deposition rates of the films were calculated from the change of films weights determined on a microbalance. Tendency for rate increase between 200 and 250 °C (from 0.3 to 0.8 nm min^{-1}), was observed, whereas above 250 °C the opposite trend was noted. The changes of the deposition parameters seems to be a consequence of: (a) the significant decrease of deposition efficiency, caused by the partial decomposition of silver species transported in the vapors, (b) deposition of metallic films on other parts of the CVD reactor (not only on substrate surfaces). XRD studies exhibit characteristic peaks of polycrystalline cubic metallic silver (38.4, 44.6, 64.7, 77.9 [deg], assigned to (1 1 1), (2 0 0), (2 2 0), (3 1 1) lines) as reported by JCPDS (International Centre for Diffraction Data) without preferential orientation.

The SEM and AFM micrographs of the films produced from **3** are presented in Fig. 6. It can be noted that at vaporization temperatures below 220 °C and deposition temperatures below 250 °C, films deposited on Si(1 1 1) substrates were composed of the separated Ag grains with diameters of 30–60 nm. Further heating resulted in coalescence of silver grains and the increase of their size (diameter 60–280 nm), as well as packing density (Fig. 6a). SEM and AFM studies of Ag films, deposited from **3** on steel substrates, under similar conditions, turned out to be very thin and dispersed, with an average grain size between 50 and 90 nm (Fig. 6b).

4. Conclusions

Analysis of variable temperature MS and IR data revealed that thermolysis of **1** and **2** proceed with complete decomposition of these compounds in the temperature range 20–250 °C. However, volatile silver containing species were not detected in the gas phase during the decomposition processes, resulting in exclusion of **1** and **2** from further thermally induced CVD experiments. Formation of volatile and stable silver–phosphine intermediates during decomposition of **3** suggested its usage as a precursor in CVD methods. However, partial decomposition of a silver bonded species during transport in the gas phase of **3** seems to be the main disadvantage in the application of this complex in metallization processes. Performed CVD experiments using **3** as a precursor proved deposition of thin silver films on Si(1 1 1) and steel substrates. In general procedures, nanometric silver films (thicknesses below 50 nm), at moderate temperature (220–250 °C) can be produced from **3**.
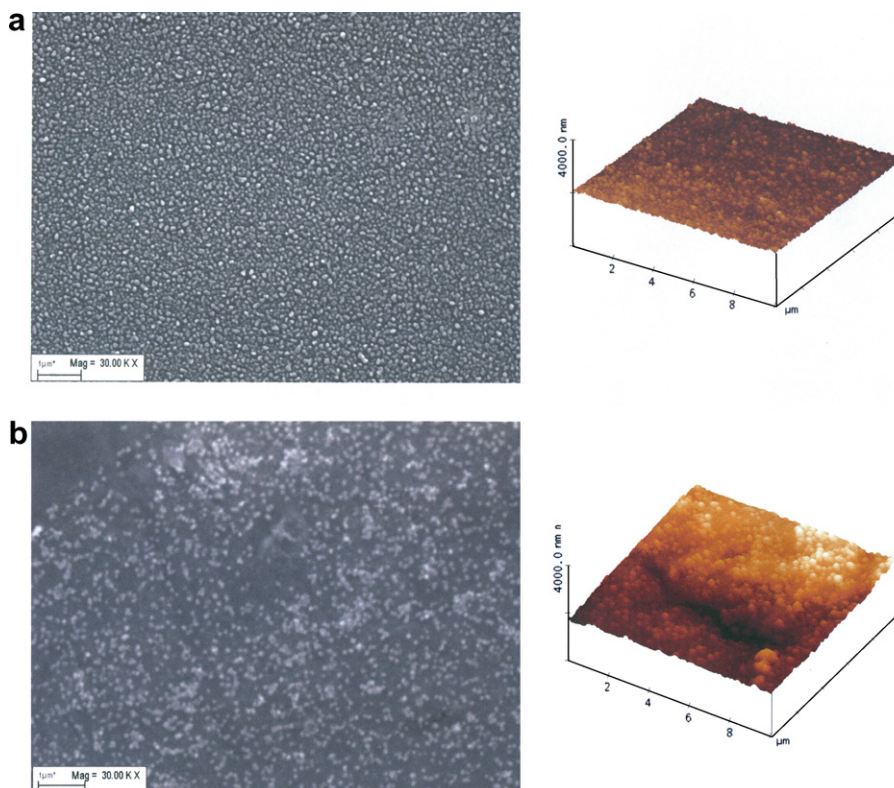
Fig. 6. SEM and AFM micrographs of silver films deposited on (a) Si(1 1 1) and (b) steel surfaces ($T_V = 170\,°C$, $T_D = 240\,°C$, $p = 2$ mbar, Ar).

Acknowledgement

References

[1] M.J. Hampden-Smith, T.T. Kodas, Adv. Mater. 7 (1995) 8.
[2] T.T. Kodas, M.J. Hampden-Smith, in: The Chemistry of Metal CVD, Weinheim, 1994.
[3] N.H. Dryden, J.J. Vittal, R.J. Pudderphatt, Chem. Mater. 5 (1993) 765.
[4] H. Schmidt, Y. Shen, M. Leschke, Th. Haase, K. Kohse-Höinghaus, H. Lang, J. Organomet. Chem. 25 (2003) 669.
[5] Z. Yuan, N.H. Dryen, J.J. Vittal, R.J. Puddephatt, Chem. Mater. 7 (1995) 1696.
[6] K. Chi, K. Chen, L. Peng, G. Lee, Organometallic 15 (1996) 2575.
[7] K.-M. Chi, Y.-H. Lu, Chem. Vap. Dep. 7 (2001) 117.
[8] A. Itsuki, H. Uchida, M. Satou, K. Ogi, Nucl. Instr. Meth. Phys. Res. B 121 (1997) 116.
[9] D.A. Edwards, R.M. Haker, M.F. Mahon, K.C. Molloy, Inorg. Chim. Acta 328 (2002) 134.
[10] E. Szłyk, P. Piszczek, A. Grodzicki, M. Chaberski, A. Goliński, J. Szatkowski, T. Błaszczyk, Chem. Vap. Dep. 7 (2001) 111.
[11] E. Szłyk, P. Piszczek, I. Łakomska, A. Grodzicki, J. Szatkowski, T. Błaszczyk, Chem. Vap. Dep. 6 (2000) 105.
[12] R.G. Goel, P. Pilon, Inorg. Chem. 17 (1978) 2876.
[13] L.S. Zheng, H.H. Yang, Q.E. Zhang, J. Struct. Chem. 10 (1991) 97.
[14] P. Rombke, A. Schier, H. Schmidbaur, S. Cronje, H. Rheimer, Inorg. Chim. Acta 357 (2004) 235.
[15] N.F. Uvarov, L.P. Burleva, M.B. Mizen, D.R. Whitcomb, C. Zou, Solid State Ionic 107 (1998) 31.
[16] L.P. Butleva, V.M. Andreev, V.V. Boldyrev, J. Therm. Anal. 33 (1988) 735.
[17] M.D. Judd, B.A. Plankett, M.I. Pope, J. Therm. Anal. 6 (1974) 555.
[18] E. Szłyk, P. Piszczek, M. Chaberski, A. Goliński, Polyhedron 20 (2001) 2853.
[19] G.D. Roberts, E. White, Org. Mass Spectrom. 12 (1981) 546.
[20] S.K. Adams, D.A. Edwards, R. Richards, Inorg. Chim. Acta 12 (1975) 163.
[21] P. Piszczek, A. Grodzicki, M. Richert, A. Radtke, Mater. Sci.-Poland 23 (2005) 663.
[22] K. Nakamoto, Infrared and Raman Spectra of Inorganic and Coordination Compounds, Wiley and Sons, 1978.
[23] G.B. Deacon, R.J. Philliphs, Coord. Chem. Rev. 33 (1980) 227.
[24] G. Wilkinson, R.D. Gillard, J.A. McClaverty, Comprehensive Coordination Chemistry, vol. 2, Pergamon Press, NY, 1987, p. 437.
[25] S.E. Paramonov, N.P. Kazumina, S.I. Troyanov, Polyhedron 22 (2003) 837.
[26] L.W. Daasch, D.C. Smith, Anal. Chem. 23 (6) (1951) 853.
[27] J. Mounier, B. Mula, A. Potier, J. Organomet. Chem. 105 (1976) 289.
[28] E. Szłyk, I. Łakomska, A. Surdykowski, A. Goliński, Pol. J. Chem. 73 (1999) 1763.
[29] E. Szłyk, I. Szymańska, R. Szczęsny, Pol. J. Chem. 79 (2005) 627.
[30] I. Łakomska, E. Szłyk, A. Grodzicki, Thermochim. Acta 315 (1998) 121.
[31] G.D. Roberts, E.V. White, Org. Mass Spectrom. 16 (1981) 564.
[32] E. Szłyk, I. Łakomska, A. Grodzicki, Thermochim. Acta 223 (1993) 207.
[33] Powder Diffraction File, Sets 4-783, International Centre for Diffraction Data (JCPDS), USA, 1977.
[34] I. Łakomska, A. Grodzicki, E. Szłyk, Thermochim. Acta 303 (1997) 41.